Biol. Cybern. 68, 275–283 (1993)

Biological Cybernetics

A neurophysiologically-based mathematical model of flash visual evoked potentials

Ben H. Jansen [1], George Zouridakis [1], Michael E. Brandt [2]

[1] Department of Electrical Engineering and Bioengineering Research Center, University of Houston, Houston, TX 77204-4793, USA
[2] Department of Psychiatry and Behavioral Sciences, University of Texas Medical School, Houston, TX 77030, USA

Received: 4 March 1992/Accepted in revised form: 27 June 1992

Abstract. Evidence is presented that a neurophysiologically-inspired mathematical model, originally developed for the generation of *spontaneous* EEG (electroencephalogram) activity, can produce VEP (visual evoked potential)-like waveforms when pulse-like signals serve as input. It was found that the simulated VEP activity was mainly due to intracortical excitatory connections rather than direct thalamic input. Also, the model-generated VEPs exhibited similar relationships between prestimulus EEG characteristics and subsequent VEP morphology, as seen in human data. Specifically, the large correlation between the N1 amplitude and the prestimulus alpha phase angle, and the insensitivity of P2 to the latter feature, as observed in actual VEPs to low intensity flashes, was also found in the model-generated data. These findings provide support for the hypothesis that the spontaneous EEG and the VEP are generated by some of the same neural structures and that the VEP is due to distributed activity, rather than dipolar sources.

1 Introduction

Very little is known about the neural substrate of most evoked potential (EP) components (Goff et al. 1978). Numerous attempts have been made to determine the location of the sources of EP activity within the brain, but these approaches generally make simplifying assumptions about the shape of the source (i.e., a dipole), the number of them, and other parameters (see Barrett 1986 for a review). There is some recent evidence (Rogers et al. 1990, 1991) that a progressive excitation of adjacent cortical columns accounts for some EP components, indicating that the EP source is not from a single neurological structure but that it is the response of a larger section of the cortex to a specific afferent input. In other words, the same neural structures that produce the spontaneous EEG activity may also be responsible for the generation of EP activity. The present study was conducted to explore this hypothesis. In this paper, we report on the degree to which the flash-visual evoked potential (VEP) can be simulated using a neurophysiologically-based mathematical model originally developed for the generation of spontaneous electroencephalogram (EEG) activity, when presented with a transient input.

In using this model, we take a system's approach to EP generation. That is, we consider the evoked potential as the output of a system excited by a transient, reflecting the volley of neural activity generated by a sensory event. This transient sums with other cortical and/or sub-cortical activity entering the same region of the cortex. At the most abstract level, the sensory input can be viewed as an impulse, and the evoked output as an impulse response. The nonlinearity of the neural networks processing the sensory input, and the fact that these networks receive sensory *and* nonsensory-related input *simultaneously*, accounts for most of the EP characteristics and variability reported in the literature. Among other things, it might account for the nonlinear interaction between visual input and the EEG in steady-state VEPs (Mast and Victor 1991), the 'augmenting' and 'reducing' responses to stimuli of different intensities (see Pineda et al. 1991 for a review), and the relationship between alpha phase at the moment of stimulation and VEP shape (Jansen and Brandt 1991).

2 Modeling of EEG and EP activity

2.1 Background

A substantial amount of literature exists on models of neural networks (see Nunez 1981; MacGregor 1987; Cotterill 1988; Koch and Segev 1989 for a review), although only a few deal with EEGs. In this context, the work by Freeman, Lopes da Silva, and Katznelson is of particular relevance.

Correspondence to: B. H. Jansen

Freeman (1975, 1987a) has attempted to model the spatial and temporal properties of potentials in the olfactory bulb through the use of a hierarchy of 'K sets'. For example, a KO set is characterized by a collection of neurons with a common input source and a common output polarity (i.e., either excitatory or inhibitory), having no functional interconnections. The KI set is a KO set with dense connections within the set. A KII set consists of interconnected KI sets, and so on. Freeman's approach starts from single neurons and can best be characterized as a local-circuit approach.

In contrast, a lumped-parameter approach was followed by Lopes da Silva et al. (1974) in their development of a model to explain the origin of alpha activity. They postulated that thalamocortical relay cells (TRCs) receive a random pulse train as input causing a postsynaptic potential (which is measurable as the scalp recorded EEG) and the firing of a new pulse train which impinges on interneurons (INs). The INs inhibit the TRCs. It was demonstrated that this negative feedback model acts as a filter, producing activity in the alpha frequency range (van Rotterdam et al. 1982). Because the TRC cells could be situated in the thalamus or in the cerebral cortex, the Lopes da Silva model may be viewed as a model of a single cortical column when an excitatory feedback loop is added (Lopes da Silva et al. 1976). (The organization of the cerebral cortex in vertically oriented columns of 200–300 μm in diameter was established by Mountcastle 1957).

Katznelson (1981) argued the importance of cortico-cortical connections of the cerebral cortex and especially the relatively long-range excitatory connections made by pyramidal neurons. He modeled the cortex as a two-dimensional spherical surface. The change in potential at any point on this surface can be determined by a set of equations, reflecting the effect of excitatory and inhibitory connections among surface regions. Katznelson linearized the input-output relation between neural mass activity and the synaptic inputs to it, in order to facilitate analytical evaluation. He showed that the model had certain normal modes (resonances), corresponding to EEG activity, including alpha and delta rhythms, depending on the selected values for the excitatory and inhibitory gain constants. Katznelson suggested (but did not give proof) that any transient input to a cortical region would elicit a series of normal modes which are linearly combined to produce an EP.

2.2 The cortical column model

The model of EEG and EP generation we explored contains components of Lopes da Silva's and Katznelson's work. We retained the nonlinearities in the cortical column model as originally proposed by Lopes da Silva and which were ignored by Katznelson. Retaining the nonlinearities means that the model can produce chaotic activity, which is important given the fact that the possible chaotic nature of various forms of EEG activity has been demonstrated by several groups of investigators (Babloyantz et al. 1985; Rapp et al. 1985; Freeman 1987b; Skarda and Freeman 1987). We followed Katznelson's lead, however, in exploring the importance of (long-range) excitatory connections by adding an excitatory feedback loop to Lopes da Silva's model. Specifically, the model is based on two interacting populations of neurons; one consisting of pyramidal cells and the other of local excitatory and inhibitory interneurons (see Fig. 1).

The linear systems labeled $h_e(t)$ and $h_i(t)$, convert axonal pulses to postsynaptic potentials. The impulse response functions $h_e(t)$ and $h_i(t)$ are shaped to resemble an excitatory postsynaptic potential (EPSP) and an inhibitory postsynaptic potential (IPSP), respectively. The input to these linear systems is *pulse density* rather than a series of single pulses. This enables us to mimic the integrating action of the soma. A static, nonlinear (sigmoidal) element ($f_e[V]$ for the pyramidal cells and excitatory interneurons, and $f_i[V]$ for the inhibitory interneurons) relates the average level of membrane potential to the pulse density of action potentials fired by the neurons. Finally, interconnectivity constants representing the average number of synaptic contacts from pyramidal cells to interneurons (C_1 and C_3), and from interneurons to pyramidal cells for both excitatory (C_4) and inhibitory (C_2) branches are used. The external pulse density $P(t)$ forms the input to the model, and consists of activity originating from adjacent and more distant cortical columns, as well as from subcortical structures (e.g., thalamus). $V(t)$ represents the membrane potential of the pyramidal cells and is to be taken as representative of the cortical EEG (Lopes da Silva and Storm van Leeuwen 1977). Interneurons receive input not only from local neuronal circuits but also from both specific and intracortical afferents (Brazier

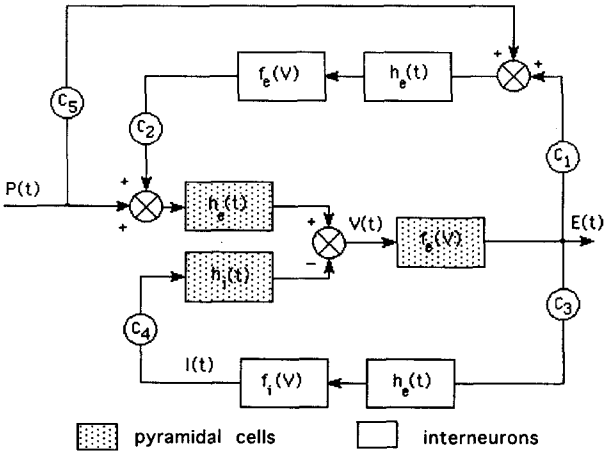

Fig. 1. Lumped parameter model for VEP generation. Two interacting populations of neurons are present: one consists of pyramidal cells and the other of local excitatory (*upper branch*) and inhibitory (*lower branch*) interneurons. $h(t)$ and $f(V)$ represent the PSP generation and the pulse-to-voltage conversion functions, respectively. Subscripts e and i are used to denote the excitatory and the inhibitory branches, respectively. C's represent the strength of the synaptic contacts from one population onto the other. $P(t)$ designates afferent activity, whereas $V(t)$ is the membrane potential which is proportional to the EEG

1964). This is taken into account by introducing a third branch into the model which – through C_5, a weighting constant – sends part of the input signal directly to the input of the excitatory loop. (This branch is active during external stimulation *only*.) In the current version of the model, a similar mechanism has not been implemented for the inhibitory loop, both for simplicity and because of the physiological evidence that inhibitory neurons receive direct afferent input through interneurons only (Andersson et al. 1971; Lopes da Silva et al. 1976; Szentágothai 1978), although other studies suggest the opposite (Toyama et al. 1974; Douglas et al. 1989).

The following expressions for the EPSP and IPSP generating blocks, originally proposed by van Rotterdam et al. (1982), have been used:

$$h_e(t) = \begin{cases} Aat\, e^{-at} & t \geqslant 0 \\ 0 & t < 0 \end{cases} \quad (1)$$

and

$$h_i(t) = \begin{cases} Bbt\, e^{-bt} & t \geqslant 0 \\ 0 & t < 0 \end{cases}, \quad (2)$$

where $A = 3.25$ mV, $B = 22$ mV, $a = 100\ s^{-1}$, and $b = 50\ s^{-1}$.

Equations (1) and (2) approximate the operation of the neuronal population in the linear range. The rate constants a and b are interpreted as being the lumped representation of the sum of the reciprocal of the time constant of passive membrane and all other spatially distributed delays, including temporal dispersion in the afferent tract, synaptic diffusion, and resistive-capacitive delay in the dendritic network (Freeman 1975). All the delays are lumped together for the sake of simplicity and because they depend mainly on structural and chemical properties of the neuron, which are relatively invariant for a given input set. (Alternatively, this impulse response can be chosen as the sum of two exponential functions as described by Freeman 1975.)

The use of (1) and (2) leads to an IPSP that is both larger in amplitude and longer in duration than an EPSP (see Fig. 2), although typically reported functions show identically shaped EPSPs and ISPSs (Curtis and Eccles 1957). In a personal communication, Lopes da Silva explained that the model was originally developed for thalamic activity and later extended to cortical alpha generation. The $h_i(t)$ used was a reasonable approximation for the one proposed by Andersen and Sears (1964) (the original thalamic data used), whereas the $h_e(t)$ was a compromise between the two forms proposed in the same article. The choice for a larger amplitude $h_i(t)$ can also be justified considering that inhibitory neurons synapse closer to the somata of pyramidal cells (often *on* the cell body) than excitatory neurons (Kandel and Schwartz 1985). This makes the effect of one inhibitory neuron about 10 times stronger than an excitatory one.

The nonlinear function $f(v)$, which represents both $f_e(v)$ and $f_i(v)$, is static and has the form of a sigmoid as

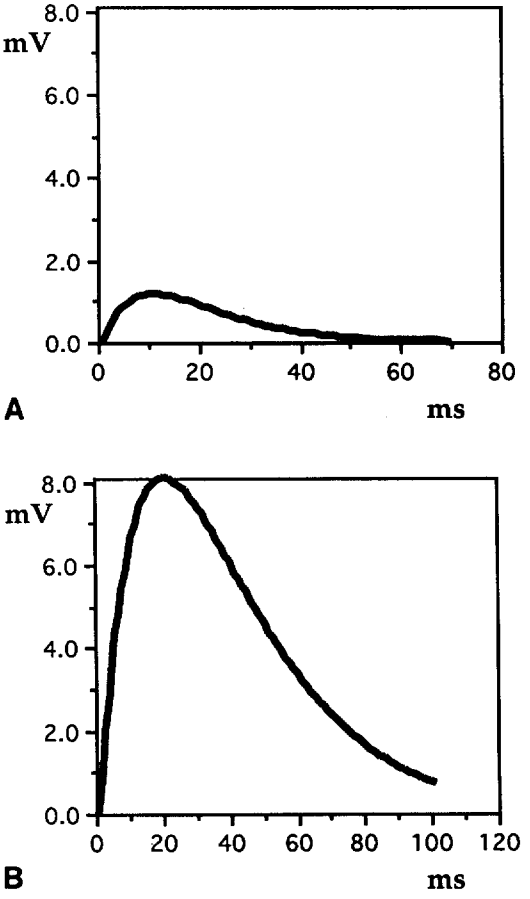

Fig. 2. A EPSP and B IPSP generating functions

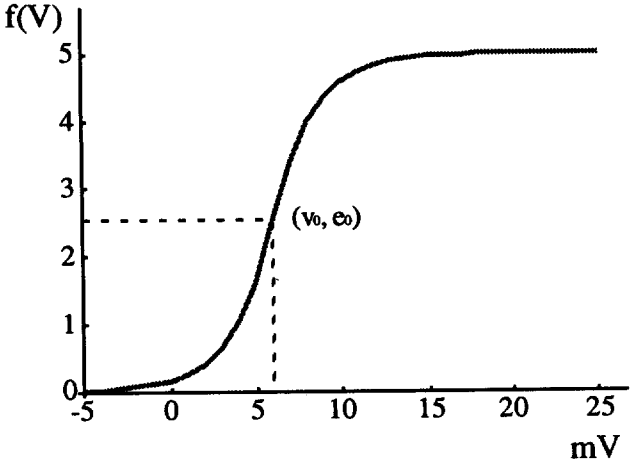

Fig. 3. Sigmoid function used for the voltage-to-pulse conversion process

depicted in Fig. 3. It is given by the following formula (Lopes da Silva et al. 1976),

$$f(v) = \begin{cases} e_0\, e^{-\gamma(v_0 - v)} & v \leqslant v_0 \\ e_0(2 - e^{-\gamma(v - v_0)}) & v > v_0 \end{cases},$$

which is very similar to one proposed by Freeman (1975). The values of the parameters are the (empiri-

cally determined, see Freeman 1987b) asymptotic maximum of the curve $2e_0 = 5.0\,s^{-1}$, and its gain $\gamma = 0.45\,mV^{-1}$. The mean firing threshold of the neural population is taken to be $v_0 = 6\,mV$.

Because of its shape, the sigmoid exhibits the recruiting mechanism that takes place when an EPSP excites a cluster of neurons with statistically distributed thresholds, and it also takes into account the presence of a refractory period (Zetterberg et al. 1978). The validity of this formula rests on the assumption that the total number of afferent fibers reaching each cell in the population is sufficiently large, for it is only in this case that all cells will be subject to approximately the same average excitation as it has been assumed in the derivation of this formula (Wilson and Cowan 1972).

As stated by Lopes da Silva et al. (1976), this model should not be considered *the* model of the EEG since the information available about various phenomena included in the scalp recorded EEG is incomplete, so that 'exact' models are elusive. Nevertheless, this model takes into consideration some of the known underlying physiological mechanisms of the cortex such as: *1)* existence of two populations of neurons (pyramidal cells and interneurons); *2)* recursion and feedback of information in an excitatory/inhibitory fashion (two lateral branches); *3)* synaptic phenomena including temporal dispersion, diffusion, and resistive-capacitive delay in the dendritic network (EPSP and IPSP functions); and *4)* linear and nonlinear interactions observed in actual neural networks.

2.3 The model input

The model input $P(t)$ in the 'spontaneous EEG'-mode is random noise, representing the effects of adjacent cortical columns and deeper brain structures. Two distinct and relatively independent mechanisms have been implemented to simulate the specific and nonspecific afferent activity elicited by, in the present case, a flash of light. The first mechanism represents activity on the *direct* channel that conveys information from the retina to the cortex through the lateral geniculate nucleus (LGN) specific afferent tract. This is modeled by adding a transient to the model input $P(t)$. The time course of this transient is based on the form and the time delay of the impulse response of the visual system. This impulse response has been determined both directly and indirectly through intracortical cell potential measurements (Brazier 1958, 1964; Kelly 1961; Watson and Nachmias 1977; Wilson et al. 1983; Fester and Lindström 1984; Ducati et al. 1988). In our model, the input function represents *pulse density* (not *membrane potential*). It has been found that in order to get a membrane potential with the characteristics previously described it is necessary that a pulse function be present at the input. Therefore, this mechanism for information transmission is modeled by a monophasic exponential function (depicted in Fig. 4A) with form and numerical values similar to the one proposed by Watson and Nachmias (1977), and given by

$$v_1 k) = q\left(\frac{k}{w}\right)^n e^{-k/w}, \tag{3}$$

with $n = 7$, $w = 5$, and $q = 0.0001$. It is this function which is added to the noise input $P(t)$.

The second mechanism represents activity on an *indirect* channel, consisting mainly of cortico-cortical afferents (both callosal and ipsilateral), and projections from higher order cortices. It also includes other subcortical projections to the cortex (such as those from non-LGN thalamic nuclei and the brainstem). The time delay on this channel is expected to be longer than the delay on the direct channel, and variable within a time range (between 90 and 100 ms). This second excitation mechanism is modeled by way of a transient increase of the excitatory connectivity constants C_1, C_2, and C_5, starting at a random delay of between 90 and 100 ms. This approach is based on the fact that EEG desynchronization is typically observed about 100 ms after the presentation of a stimulus and is related to in-

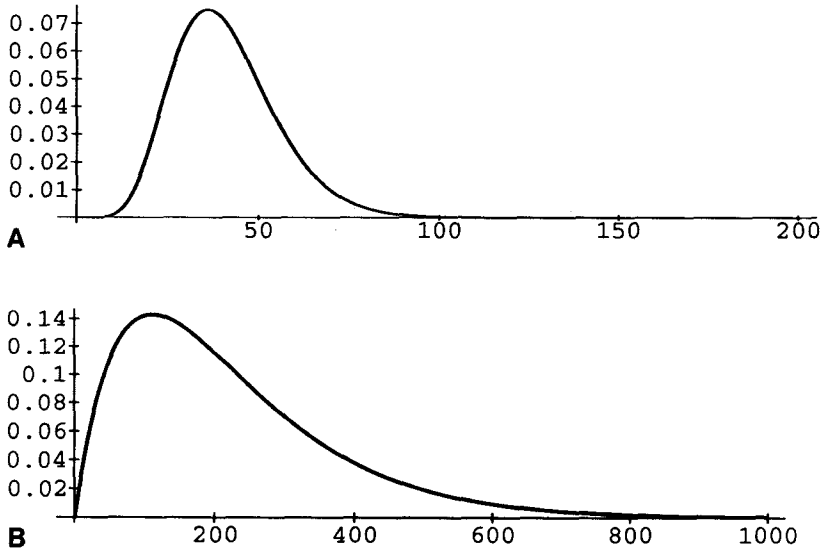

Fig. 4. **A** Excitation function due to specific afferent input. **B** Excitation function due to nonspecific afferent input

creased excitability (Steriade and Llinàs 1988). Thus, the second excitation mechanism accounts mostly for the increased cortical activity due to the recruiting mechanism known to take place. It is not necessary to make similar changes in the inhibitory branch because inhibitory mechanisms are thought to be blocked during EEG desynchronization (Steriade and Llinàs 1988). The function we used (shown in Fig. 4B) is, again, a monophasic version of the one proposed by Watson and Nachmias (1977), given by

$$v_2(k) = \alpha k \, e^{-dk}, \tag{4}$$

with $\alpha = 0.0035$, and $d = 0.01$. Starting at a random delay of between 90 and 100 ms the function v_2 is added to the connectivity constants C_1, C_2, and C_5.

3 Results

The model produced[1] alpha-like activity for connection coefficients set at $C_1 = C_2 = 0.05$, $C_3 = 0.08$, and $C_4 = 0.06$. The input noise $P(t)$ had a mean value of 2.4 and a standard deviation of 2.0. A detailed description of the model behavior as a function of these model parameters can be found in Zouridakis (1990) and will be the subject of another paper.

A single-trial VEP consisted of one second of prestimulus EEG followed by one second of poststimulus activity. In order to investigate the relationship between the phase of the prestimulus alpha activity and the shape of the resulting VEP, selective averaging of single trials was performed. The procedure used to generate the simulated VEPs was similar to the one applied to human data (Brandt 1989; Jansen and Brandt 1991). Specifically, the phase of the alpha rhythm at the time of stimulation was divided into eight groups (numbered from 0 to 7) with a 45 degrees phase difference between successive groups (see inset, Fig. 5). Single-trial VEPs were, then, clustered on the basis of this phase angle.

The model was set to produce alpha activity, and after one second (1000 iterations), a stimulus, as described in the preceding section, was presented at a specific alpha-phase angle. Subsequent stimuli were separated by three-second intervals, thus the model was allowed enough time to return to steady state. The state of the system at the end of a trial formed the initial conditions of the following iteration, i.e., the model was not re-initialized at the beginning of each trial.

There is a slight difference between human and simulated data in the way the phase was controlled. In the human data, stimuli were presented in a pseudo-random manner, and the phase of the alpha activity at the moment of stimulation was determined a posteriori. Consequently, the phase angles of the trials in, say, phase category 6, were more or less uniformly distributed between $3\pi/8$ and $5\pi/8$. In the simulated data, however, the phase angle was determined a priori, hence, all stimuli in a specific phase category were presented at exactly the same phase (e.g., $3\pi/8$ for category 6 and $5\pi/8$ for category 7).

A complete set of eight selectively averaged VEP responses, as produced by the model, is shown in Fig.

[1] All simulations were done using the forward Euler multi-step technique, with a sampling interval of 1 ms

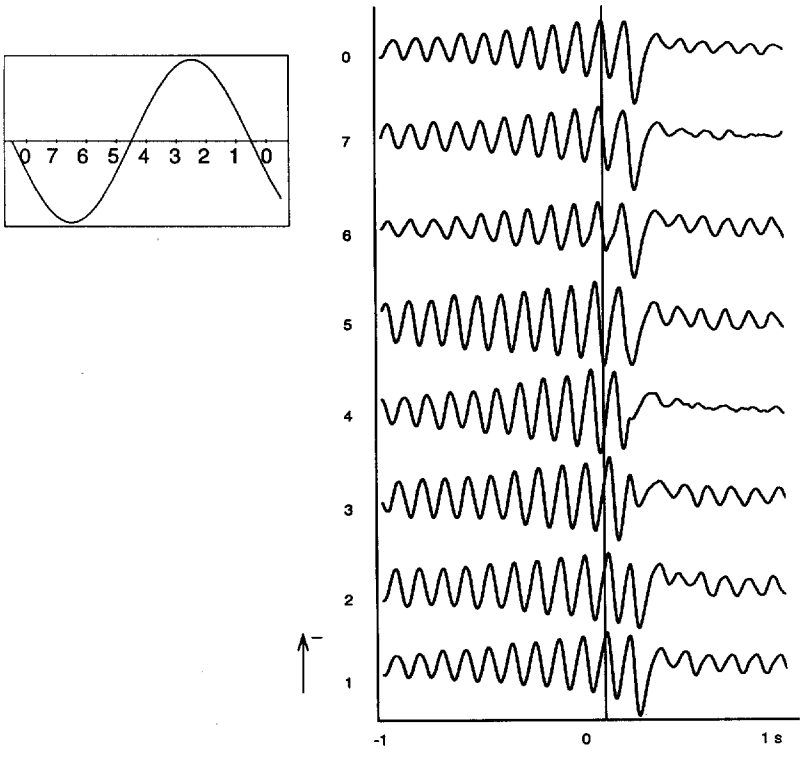

Fig. 5. VEPs produced by the model as a function of the phase angle of the alpha activity at the time of stimulation. Monopolar recordings. The phase angle classes are indicated in the inset

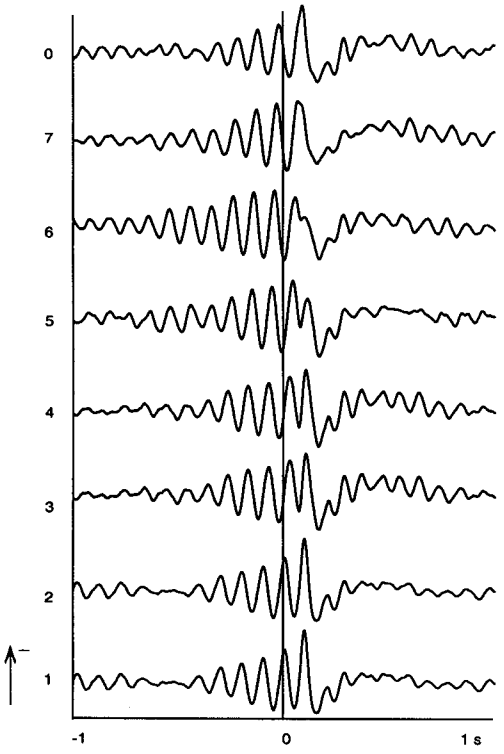

Fig. 6. VEP responses obtained from a human subject. The indicated phases correspond to the phase angles shown in the inset of Fig. 5

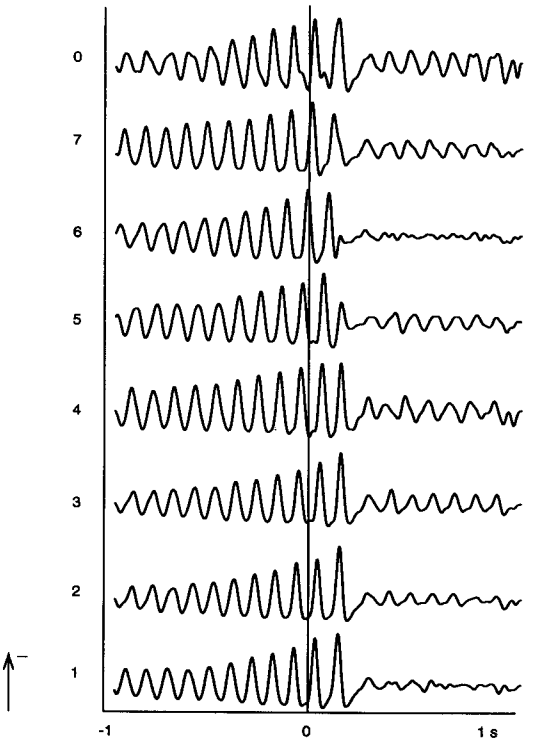

Fig. 7. VEPs produced by the model. Bipolar recordings. The numbers correspond to the phase angles shown in the inset of Fig. 5

5. A similar set for human VEP data is shown in Fig. 6. Each trace in these figures depicts one second of prestimulus and one second of poststimulus activity. The time of stimulation is indicated by a vertical line (designated as time zero on the horizontal axis). The numbers on the left indicate the phase angles used to group the corresponding traces.

The output signal produced by the model is comparable to the intracortical membrane potential, and represents monopolar activity in its purest form, i.e., with one electrode over the electrically active site and the second electrode at infinity. For this reason, further processing was required to produce a signal similar to scalp-recorded EEG. We hypothesize that this processing is essentially a differentiation process, in analogy to the relationship between membrane voltages in heart-muscle tissue and the surface-recorded electrocardiogram (ECG). A 'noisy' approximation of this operation is obtained by replacing the output samples by the difference between two successive samples in the sequence. The effect of the noise that this approach introduces was reduced by low-pass filtering. The latter also simulates the filtering effect due to the meningi, skull and scalp on the electrocorticogram. The low-pass operation was implemented with a zero-phase (IIR, 'bidirectional') filter with cut-off frequency set at 35 Hz. Figure 7 shows the VEPs obtained after applying the aforementioned differentiation and low-pass filtering procedure to the signals shown in Fig. 5.

A global similarity is apparent between the human and simulated data, as can be seen by comparing Figs. 6 and 7. Notice that beginning 1 s before the onset of the stimulus, the prestimulus activity is synchronized alpha and increases as the moment of stimulation approaches. This is true in all cases and is expected based on the autocorrelation function of alpha activity, since selective averaging of single trials resembles an autocorrelation function computation, which assumes its maximum value at time zero. However, for most phase angles, the alpha amplitude increases even after the onset of the stimulus and reaches a maximum at a latency that corresponds to that of the N1 component.

The most negative deflection around 100 ms poststimulus was taken as the N1. There is a strong influence of the alpha phase on this component. In the simulated data the maximum N1 is attained for phase number 1, and its minimum for phase number 7. In human data, on average, these phases correspond to 2 and 6 (over 7 subjects and 16 data sets) (Jansen and Brandt 1991), respectively. Also the latency of N1 shows some variation. Minimum and maximum N1 latencies are reached at phases 7 and 5, respectively, in the human data set and at 6 and 5 in the simulated data set.

Another similarity between the human and simulated data is that approximately 120–140 ms after the presentation of the stimulus (at a latency that corresponds to the beginning of the P2 component, i.e., the second positive peak), a rather drastic change in the pattern of the VEP takes place and the alpha activity is highly reduced (in the simulated data the oscillatory pattern disappears), whereas later activity, after about

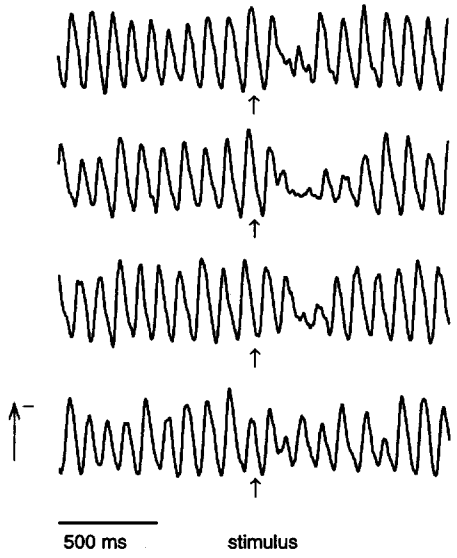

Fig. 8. Simulated single-trial VEPs demonstrating alpha blocking approximately 120 ms poststimulus

another 140 ms, is again oscillatory and falls in the alpha band. This 'alpha blocking' is visible also on a single trial basis as Fig. 8 shows, indicating that the alpha reduction seen in the VEP actually takes place and is not the result of averaging (due, for example, to lack of synchronization).

Interestingly, the latency of occurrence of the positive peak in the P2 range seems to be unaffected by the phase angle of stimulation in both human and simulated data. Its amplitude, however, as peak-to-peak measurement reveals, does depend on the phase of the alpha rhythm at the time of stimulation and assumes its largest value at phase 2 for both human and simulated data. Also, the average poststimulus activity does not have the same amplitude for all phase angles. Phases 1, 2 and especially 6 show lower amplitude. In our human data set, low amplitude poststimulus activity corresponded to phases 2 and 5. Beyond the similarities between actual and simulated data, some obvious differences do exist. For instance, in the case of human data the transition from 'alpha blocked' to 'alpha re-instated' is much smoother, and a transitional oscillation between the two states is present. In the simulated data, this transition is completed in one step, i.e., the positive P2 peak is followed almost immediately by the oscillatory alpha pattern. In order to de-couple the effect of the two simultaneously occurring types of stimulation (i.e., the presentation of a pulse at the input and the changes effected by varying C_5, C_2 and C_1), the procedure that generates VEPs was repeated with the exception that now the model was given a stimulus at the input only. That is, only the function depicted in Fig. 4A was activated while the excitatory connectivity constants remained fixed during the course of the experiment. All other functions and parameter values remained the same. This type of stimulation would account for the hypothetical case whereby a neuronal column receives only (specific afferent) input from the LGN and there is

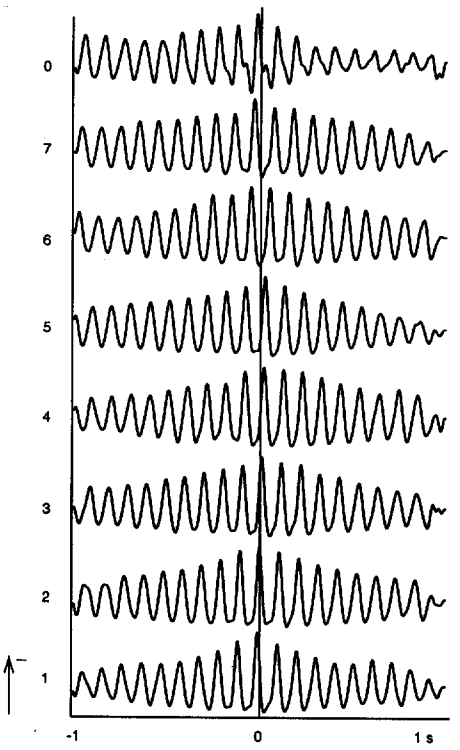

Fig. 9. VEPs produced by the model with a direct excitation stimulus only at the input. Again, the numbers correspond to the phase angles shown in the inset of Fig. 5

no interaction with adjacent columns or other subcortical structures. Figure 9 summarizes the results obtained.

As one can see, there is little difference between the pre- and poststimulus averaged activity, and there is little evidence of evoked potential activity at all.

In a different set of experiments, only random noise was given at the input. Thus, the model was excited only indirectly by way of varying the excitatory connectivity constants C_1, C_2, and C_5 using the function given by (4). The effect of each of these parameters was studied by activating either C_5 only, C_1 and C_2 only, or C_1, C_2, and C_5 simultaneously. These experiments would account for the (again) hypothetical situation whereby only nonspecific afferent input is present. It was found that an increase of C_5 only (i.e., an increase in subcortical-to-cortical connections only) had very little effect on the evoked response. On the other hand, VEPs produced by increasing either C_1 and C_2 only, or C_1, C_2, and C_5 simultaneously are practically the same as those shown in Fig. 7 (obtained with both direct and indirect excitation), suggesting that the response can be attributed mainly to the excitatory constants C_1 and C_2, i.e., to intracortical excitatory connections, which is in accordance with microanatomical data presented by Douglas et al. (1989).

4 Conclusions

Ongoing EEG activity (in particular the alpha rhythm) has been successfully modeled by means of a nonlinear,

lumped-parameter model representing localized cortical activity. This model, originally developed by Lopes da Silva et al. (1974, 1976), takes into account some dynamical characteristics of the brain. Our slightly modified version includes a direct excitatory branch through C_5, and makes use of new values for the connectivity constants C_1 through C_4. When subjected to appropriate stimulation, the model is capable of producing VEP-like waveforms having a phenomenological global similarity to actual EEG/VEP recordings. The major findings regarding VEP generation are summarized below.

When stimuli are synchronized with a specific phase angle of the prestimulus alpha activity, one observes that the prestimulus alpha activity appears to continue into the N1 latency range. The amplitude of this activity seems to increase even after the onset of the stimulus and reaches a maximum at phase 0 that corresponds to the positive zero-crossing. This increase could be explained as resulting from an increase in the excitatory branch of the network due to the particular nature of the indirect stimulus. However, the increase observed in the amplitude of the VEP takes place well before the indirect excitation in the model is activated (the latter kicks in *at least* 90 ms after the direct-stimulus onset, see Sect. 2.3). Thus, such a possibility has to be discarded. Another possibility could be the direct stimulus which is added to the input. Yet, we have found that an increase of the mean value of the input of the model results in a decrease of the output (Zouridakis 1990), therefore this option has to be discarded, too. Alternatively, it can be hypothesized that a *phase reorganization* takes place after the arrival of the stimulus, i.e., the stimulus resets the phase of the output signal. This same phenomenon was seen in a model for hippocampal neuronal activity (Traub et al. 1988), whereby a brief stimulus was capable of resetting the output phase. Such phase reorganizational behavior is quite common in nonlinear systems and has been observed in several biological oscillators as well (Winfree 1987; Glass and Mackey 1988). Our studies suggest that similar behavior is observed in the cortical EEG.

The N1 component was found not to be due to direct thalamic input; rather it was the result of a gradual activation of excitatory intracortical connections. This is in accordance with the physiological data and the model predictions reported by Douglas et al. (1989), whereby a simplified circuit of the cat striate cortex was developed based on intracellular in vivo recordings. Similar results are shown in a recent study of auditory EPs obtained via evoked magnetic-field recordings, in which a dynamic excitation pattern of adjacent columns was suggested as the source of the auditory N1m component (i.e., the magnetic equivalent of N1) (Rogers et al. 1990). Our model predicts this mechanism for N1 generation, in the sense that the EP activity generated in our model is primarily due to adjacent cortical columns.

The poststimulus activity undergoes a drastic reduction in amplitude at a latency that corresponds to the beginning of P2, and it is fully re-instated about 200 ms poststimulus. The appearance of the model-generated P2 is directly related to the form of the excitation function which allows for a brief, high increase in the excitatory branch that drives the system temporarily to saturation which, in turn, results in the absence of the oscillatory output. However, as this function decreases, the system output returns to the oscillatory pattern. This transition in human data is smoother than in the simulated data and the change between the states 'alpha blocked' and 'alpha re-instated' is more gradual. Thus, the P2 component accessed in our data was actually only a positive-going peak at that latency and not a full component. In physiological terms this would imply that a more complex mechanism is involved in the excitation process and the consequent appearance of P2.

Since alpha activity is blocked at the time that corresponds to the P2 latency, the latter is expected to be unaffected by prestimulus alpha characteristics. It turns out that the latency of this component is not affected by the phase angle of the alpha at the time of stimulation. Its amplitude, however, was found to reach a maximum value at phase 2 and a minimum at phase 6. Brandt's (1989) results show a maximum value at phases corresponding to the negative zero-crossing (numbers 3, 4, and 5). Again, this discrepancy suggests that late components, such as the P2, may be due to different excitation processes, involving larger regions of the brain.

The major contributor to the model-generated VEP is the excitation function that involves the connectivity constants C_1, C_2, and C_5. This is in accordance with the neurophysiological fact that the effect of excitation is exerted mainly (but not only) on interneurons rather than on pyramidal cells directly (Brazier 1964; Szentágothai 1978).

In conclusion, these studies strongly suggest that the neurophysiological structures responsible for the generation of spontaneous EEG (and especially, alpha activity) are also involved in the generation of the VEPs. For a more direct test of the moving dipole hypothesis we intend to interconnect a number of cortical column models (rather than increasing the excitatory feedback gain). By making some (or all) of the cortical columns sensitive to specific stimulus properties only (for example, some column models respond only to vertical lines and others to horizontal line segments), it will be possible to explore Katznelson's hypothesis that the particular set of normal modes that are excited (and give rise to different EPs) depend on the manner and spatial extent of the delivered stimulus.

References

Andersen P, Sears TA (1964) The role of inhibition in the phasing of spontaneous thalamo-cortical discharges. J Physiol 173:459–480

Andersson SA, Holmgren E, Manson JR (1971) Localized thalamic rhythmicity induced by spinal and cortical lesions. Electroencephal Clin Neurophysiol 31:347–356

Babloyantz A, Salazar JM, Nicolis C (1985) Evidence of chaotic dynamics of brain activity during the sleep cycle. Phys Lett 111A:152–156

Barrett G (1986) Analytic techniques in the estimation of evoked potentials. In: Lopes da Silva LH, Storm van Leeuwen W, Rémond A (eds) Clinical applications of computer analysis of EEG and other neurophysiological signals. Elsevier Scientific Publishers, Amsterdam, pp 311–333

Brandt ME (1989) The relationship between prestimulus EEG and visual evoked potentials. Ph.D.-dissertation, Biomedical Engineering Program, University of Houston, Houston

Brazier MAB (1958) Studies of evoked responses by flash in man and cat. In: Reticular formation of the brain. Little Brown & Co., Boston, pp 151–176

Brazier MAB (1964) Evoked responses recorded from the depths of the human brain. Ann NY Acad Sci 112:33–59

Cotterill RMJ (ed) (1988) Computer simulation in brain science. Cambridge University Press, Cambridge

Curtis DR, Eccles JC (1957) The time course of excitatory and inhibitory synaptic action. J Physiol 145:522

Douglas RJ, Martin KAC, Whitteridge D (1989) A canonical microcircuit for neocortex. Neural Computat 1:480–488

Ducati A, Fava E, Motti EDF (1988) Neuronal generators of the visual evoked potentials: intracerebral recordings in awake humans. Electroencephal Clin Neurophysiol 71:89–99

Fester D, Lindström S (1984) Neuronal circuitry of the cat visual cortex. In: Edelman GM, Gall WE, Cowan WM (eds) Dynamic aspects of neocortical function. John Wiley, New York, pp 87–103

Freeman WJ (1975) Mass action in the nervous system. Academic Press, New York

Freeman WJ (1987a) Analytic techniques in the search for the physiological basis of the EEG. In: Gevins AS, Rémond A (eds) Methods of analysis of brain electrical and magnetic signals. EEG Handbook, vol 1. Elsevier, Amsterdam

Freeman WJ (1987b) Simulation of chaotic EEG patterns with a dynamical model of the olfactory system. Biol Cybern 56:139–150

Glass L, Mackey MC (1988) From clocks to chaos, the rhythms of life. Princeton University Press, Princeton

Goff WR, Allison T, Vaughan Jr HG (1978) The functional neuroanatomy of the event-related potentials. In: Callaway E, Tueting P, Koslow SH (eds) Event-related brain potentials in man. Academic Press, New York, pp 1–79

Jansen BH, Brandt ME (1991) The effect of the phase of prestimulus alpha activity on the averaged visual evoked response. Electroencephal Clin Neurophysiol 80:241–250

Kandel ER, Schwartz JH (1985) Principles of neural science. Elsevier, Amsterdam

Katznelson RD (1981) Normal modes of the brain: neuroanatomical basis and a physiological theoretical model. In: Nunez P (ed) Electric fields of the brain: the neurophysics of EEG. Oxford University Press, New York, pp 401–442

Kelly DH (1961) Visual response to time-dependent stimuli. II. Single-channel model of the photopic visual system. J Opt Soc Am 51: 747–754

Koch C, Segev I (eds) (1989) Methods in neuronal modeling: from synapses to networks. MIT Press, Cambridge

Lopes da Silva FH, Hoeks A, Zetterberg LH (1974) Model of brain rhythmic activity. Kybernetik 15: 27–37

Lopes da Silva FH, Rotterdam A van, Barts P, Heusden E van, Burr W (1976) Model of neuronal populations. The basic mechanism of rhythmicity. In: Corner MA, Swaab DF (eds) Progress in brain research, vol 45. Elsevier, Amsterdam, pp 281–308

Lopes da Silva FH, Storm van Leeuwen W (1977) The cortical sources of the alpha rhythm. Neurosci Lett 6:237–241

MacGregor RJ (1987) Neural and brain modeling. Academic Press, New York

Mast J, Victor JD (1991) Fluctuations of steady-state VEPs: Interaction of driven evoked potentials and the EEG. Electroencephal Clin Neurophysiol 78:389–401

Mountcastle VB (1957) Modality and topographic properties of single neurons of cat's somatic sensory cortex. J Neurophysiol 20: 408–434

Nunez PL (1981) Electric fields of the brain: the neurophysics of EEG. Oxford University Press, New York

Pineda JA, Holmes TC, Foote SL (1991) Intensity-amplitude relationships in monkey event-related potentials: parallels to human augmenting-reducing responses. Electroencephal Clin Neurophysiol 78:456–465

Rapp PE, Zimmerman ID, Albano AM, deGuzman GC, Greenbaum NN, Bashore TR (1985) Experimental studies of chaotic neural behavior: cellular activity and electroencephalographic signals. In: Othmer HG (ed) Nonlinear oscillations in biology and chemistry. Springer, Berlin Heidelberg New York, pp 175–205

Rogers RL, Papanicolaou AC, Baumann SD, Sydjarï C, Eisenberg HM (1990) Neuromagnetic evidence of a dynamic excitation pattern generating the N100 auditory response. Electroencephal Clin Neurophysiol 77:237–240

Rogers RL, Baumann SD, Papanicolaou AC, Bourbon TW, Alagarsamy S, Eisenberg HM (1991) Localization of the P3 sources using magnetoencephalography and magnetic resonance imaging. Electroencephal Clin Neurophysiol 79:308–321

Rotterdam A van, Lopes da Silva FH, van den Ende J, Viergever MA, Hermans AJ (1982) A model of the spatial-temporal characteristics of the alpha rhythm. Bull Math Biol 44:283–305

Skarda A, Freeman WJ (1987) How brains make chaos in order to make sense of the world. Behav Brain Sci 10:161–195

Steriade M, Llinàs R (1988) The functional states of the thalamus and the associated neuronal underplay. Physiol Rev 68: 649–742

Szentágothai J (1978) The local neuronal apparatus of the cerebral cortex. In: Cerebral correlates of conscious experience. Elsevier/North Holland Biomedical Press, Amsterdam, pp 131–138

Traub RD, Miles R, Wong RKS (1988) Large scale simulations of the hippocampus. IEEE Eng Med Biol 7:31–38

Toyama K, Matsunami K, Ohno T, Tokashiki S (1974) An intracellular study of neuronal organization in visual cortex. Exp Brain Res 21:45–66

Watson AB, Nachmias J (1977) Patterns of temporal integration in the detection of grating. Vision Res 17:893–902

Wilson HR, Cowan JD (1972) Excitatory and inhibitory interaction in localized populations of model neurons. Biophys J 12:1–24

Wilson CL, Babb TL, Halgren E, Crandall PH (1983) Visual receptive fields and response properties of neurons in human temporal lobe and visual pathways. Brain 106:473–502

Winfree AT (1987) When time breaks down. Princeton University Press, Princeton

Zetterberg LH, Kristiansson L, Mossberg K (1978) Performance of a model for a local neuron population. Biol Cybern 31:15–26

Zouridakis G (1990) Nonlinear modeling of EEG and VEP activity. M.Sc.-Thesis, Biomedical Engineering Program, University of Houston, Houston